A 2-D Time-Domain BIEM for Dynamic Analysis of Cracked Orthotropic Solids [1]

Ch. Zhang[2]

Abstract: A 2-D time-domain boundary integral equation method (BIEM) for transient dynamic analysis of cracked orthotropic solids is presented in this paper. A finite crack in an unbounded orthotropic solid subjected to an impact loading is considered. Hypersingular time-domain traction boundary integral equations (BIEs) are applied in the analysis. A time-stepping scheme is developed for solving the hypersingular time-domain traction BIEs. The scheme uses a convolution quadrature formula for temporal and a Galerkin method for spatial discretizations. Numerical examples are given to show that the presented time-domain BIEM is highly efficient and accurate.

keyword: Time-domain boundary integral equation method, 2-D orthotropic solids, elastodynamic crack analysis, elastodynamic stress intensity factors.

1 Introduction

Though the time-domain boundary element method (BEM) has been successfully applied to dynamic analysis of isotropic solids for many years, its applications to anisotropic solids are yet still very limited. This is due to the lack of closed or simple form elastodynamic Green's functions for anisotropic solids, which influences the efficiency of the time-domain BEM significantly (Beskos, 1997). Recent effort toward developing simple form time-domain and frequency-domain Green's functions for anisotropic solids has been presented by Wang and Achenbach (1992, 1993, 1994, 1995). For elastodynamic analysis of anisotropic solids, different BEM formulations can be found in literature. The first one is the so-called dual reciprocity BEM, either in time-domain (see e.g. Albuquerque and Sollero, 1998; Albuquerque, Sollero, and Aliabadi, 1999a, 1999b, 2000;

Kögl and Gaul, 2000) or in Laplace transform domain (see e.g; Albuquerque, Sollero, and Fedelinsky, 2000). The dual reciprocity BEM applies static Green's functions, which have simple forms, and avoids the use of complicated time-domain Green's functions. The second one is the conventional time-domain BEM by using time-dependent Green's functions (see e.g. Hirose, 1999; Hirose, Wang, and Achenbach, 2000; Nishimura, Kobayashi, and Kishima, 1986; Nishimura, Kobayashi, and Takeuchi, 1995; Wang, Achenbach, and Hirose, 1996; Zheng and Dravinski, 2000). The third method is the frequency-domain BEM which solves the boundary value problem in the frequency-domain (see e.g. Dominguez and Sáez, 1998; Mattsson, 1996; Sáez and Dominguez, 1999a, 1999b, 2000, 2001; Wang, Sáez, and Achenbach, 1995). Recently, Zhang (2000a, 2000b) presented a time-domain traction BIEM for cracked anisotropic solids where the convolution quadrature formula of Lubich (see e.g. Lubich, 1988a, 1988b, 1994; Lubich and Schneider, 1992) is adopted for temporal discretization of the time-domain traction BIEs and only Laplace-domain Green's functions are needed. For spatial discretization of the time-domain traction BIEs, Zhang (2000a, 2000b) applied a Galerkin method. Each of the above mentioned methods has its advantages and drawbacks. The dual reciprocity BEM avoids the use of complicared time-domain Green's functions but involves internal nodes which may be not suitable and less accurate for unbounded solids. In addition, the applicability of the dual reciprocity BEM to wave scattering analysis in unbounded domains for computing the scattered far filed is questionable, since the radiation conditions for scattered waves at infinty are not ensured automatically. The conventional time-domain BEM applies in general very complicated time-domain Green's functions, which are difficult for numerical implementation and reduce hence the efficiency of the time-domain BEM. Besides, the choice of the time-step is crucial in the conventional time-domain BEM: a too small time-step may lead to numerical instability of the time-stepping scheme, while

---

[1] This paper is dedicated to Prof. Dr.-Ing. D. Gross, Technical University Darmstadt, Germany, on the occasion of his 60th birthday

[2] Department of Civil Engineering, Hochschule Zittau/Görlitz, University of Applied Sciences, D-02763 Zittau, Germany.

a too large time-step may cause unreasonable numerical damping of the results. The frequency- or Laplace-domain BEM has the advantage that it utilizes frequency- or Laplace-domain Green's functions which are easy to obtain and have in most cases a simple mathematical structure. Through Fourier or Laplace inverse transform, stable numerical results at large-time can be obtained, but the method may be very inaccurate in the short-time range for impact loaded solids. The time-domain BIEM for anisotropic solids by using the convolution quadrature formula of Lubich (see e.g. Lubich, 1988a, 1988b, 1994; Lubich and Schneider, 1992) for temporal discretization as presented by Zhang (2000a, 2000b) combines the advantages of the conventional time-domain BEM and the Laplace-domain BEM: its formulation is directly in the time-domain, but it requires only the simple Laplace-domain Green's functions, and it is highly accurate and much more stable than the conventional time-domain BEM.

In this paper, a 2-D BIEM is presented for transient elastodynamic analysis of cracked orthotropic solids. A hypersingular time-domain traction BIE formulation is used for this purpose, in which the crack-opening-displacements (CODs) are the fundamental unknown quantities. To solve the hypersingular time-domain traction BIEs, a time-stepping scheme is developed. In comparison to the commonly applied time-domain BEM/BIEM for anisotropic solids, the present method contains two novel aspects:

- *Approximation of the temporal convolution* of the time-domain traction BIEs by the convolution quadrature formula of Lubich (see e.g. Lubich, 1988a, 1988b, 1994; Lubich and Schneider, 1992). In the convolution quadrature method, a multistep method is used and only Laplace-domain elastodynamic Green's functions are required. The Laplace-domain elastodynamic Green's functions for orthotropic solids can be expressed as Fourier integrals and have a simple mathematical structure.

- *Approximation of the spatial variation* of the crack-opening displacements (CODs) by a Galerkin-ansatz in terms of Chebyshev polynomials, which can properly describe the local square-root behavior of the CODs at crack-tips. The application of a spatial Galerkin method to the time-domain traction BIEs leads to a system of linear algebraic equations

for the unknown expansion coefficients. A time-stepping scheme is developed for solving the linear algebraic equations.

One important feature of the present time-domain traction BIEM is that it requires no special technique for integrating the arising hypersingular integrals. Another interesting feauture of the method is that the triple integrals appearing in the spatial Galerkin method can be reduced to a single integral like in the collocation method, which reduces the numerical expenses, improves the accuracy of the Galerkin method, and makes the method especially attractive.

Elastodynamic stress intensity factors are computed directly from the numerically calculated CODs. Numerical examples are presented to show the accuracy, efficiency and stability of the method. In the special case of isotropy, numerical results are also given and compared with the analytical results of Thau and Lu (1971). Numerical results for a finite crack in an unbounded orthotropic solids are presented and compared with the numerical results of Kassir and Bandyopadhyay (1983). In addition, numerical results for several values of the material anisotropy parameter are given to analyze its effects on elastodynamic stress intensity factors.

A spectral scheme for dynamic fracture analysis of composites was developed by Hwang and Geubelle (2000). BEM was applied by Shiah and Tan (2000) for fracture mechanics analysis in 2-D anisotropic thermoelastic solids.

2 Problem Formulation and Time-Domain BIEs

Let us consider a straight finite crack of length $2a$ in an unbounded, homogeneous, linearly elastic, and orthotropic solid as shown in Fig. 1. The cracked or-
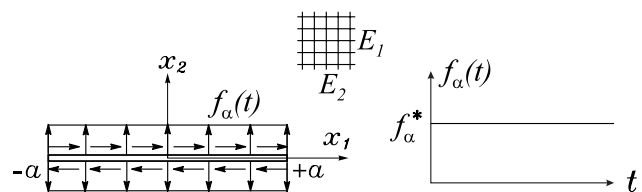
Figure 1 : A finite crack in an unbounded orthotropic solid

thotropic solid is subjected to an impact loading on the

crack-faces, and the deformation of the solid is assumed to be in a state of generalized plane strain or generalized plane stress. In the absence of body forces, the cracked orthotropic solid satisfies the equations of motion (see Achenbach, 1973)

$$\sigma_{\alpha\beta,\beta} = \rho \ddot{u}_\alpha, \tag{1}$$

the Hooke's law

$$\begin{Bmatrix} \sigma_{11} \\ \sigma_{22} \\ \sigma_{12} \end{Bmatrix} = \begin{bmatrix} C_{11} & C_{12} & 0 \\ C_{21} & C_{22} & 0 \\ 0 & 0 & C_{66} \end{bmatrix} \begin{Bmatrix} \varepsilon_{11} \\ \varepsilon_{22} \\ 2\varepsilon_{12} \end{Bmatrix}, \tag{2}$$

the initial conditions

$$u_\alpha(\mathbf{x},t) = \dot{u}_\alpha(\mathbf{x},t) = 0, \quad \text{for} \quad t = 0, \tag{3}$$

and the traction boundary conditions on the crack-faces

$$\sigma_{\alpha\beta}(\mathbf{x},t)n_\beta(\mathbf{x}) = f_\alpha(\mathbf{x},t), \quad \mathbf{x} \in \Gamma_c. \tag{4}$$

Here, $\sigma_{\alpha\beta}$, $\varepsilon_{\alpha\beta}$ and u_α denote the stress, the strain and the displacement components, ρ is the mass density, C_{ij} $(i,j = 1,2,6)$ is the elasticity matrix, $f_\alpha(\mathbf{x},t)$ is the traction vector, n_β is the unit normal vector, and $\Gamma_c = \Gamma_c^+ + \Gamma_c^-$ are the upper and lower crack-faces, respectively. A comma after a quantity stands for partial derivatives with respect to spatial variables, while superscript dots represent temporal derivatives with respect to time. Also, the conventional summation rule over double indices is implied, and Greek indices take the values 1 and 2. For orthotropic solids, the elasticity matrix C_{ij} is related to the engineering elastic constants by

$$\begin{bmatrix} \frac{E_1}{1-\nu_{12}\nu_{21}} & \frac{\nu_{12}E_2}{1-\nu_{12}\nu_{21}} & 0 \\ \frac{\nu_{12}E_2}{1-\nu_{12}\nu_{21}} & \frac{E_2}{1-\nu_{12}\nu_{21}} & 0 \\ 0 & 0 & G_{12} \end{bmatrix} \tag{5}$$

for generalized plane stress, and

$$\begin{bmatrix} \frac{E_1}{\Delta}(1-\nu_{23}\nu_{32}) & \frac{E_1}{\Delta}(\nu_{21}+\frac{E_2}{E_1}\nu_{13}\nu_{32}) & 0 \\ \frac{E_1}{\Delta}(\nu_{21}+\frac{E_2}{E_1}\nu_{13}\nu_{32}) & \frac{E_2}{\Delta}(1-\nu_{13}\nu_{31}) & 0 \\ 0 & 0 & G_{12} \end{bmatrix} \tag{6}$$

for generalized plane strain, where

$$\Delta = 1 - \nu_{12}\nu_{21} - \nu_{23}\nu_{32} - \nu_{31}\nu_{13} - \nu_{12}\nu_{23}\nu_{31} - \nu_{13}\nu_{21}\nu_{32}. \tag{7}$$

Here, E_1 and E_2 are Young's muduli, ν_{12}, ν_{21}, ν_{13}, ν_{23}, ν_{31} and ν_{32} are Poission's ratios, G_{12} is the shear modulus, and the following relation holds

$$\nu_{12}E_2 = \nu_{21}E_1. \tag{8}$$

The displacement field can be represented by a boundary integral as

$$u_\gamma(\mathbf{x},t) = \int_{\Gamma_c^+} \sigma_{\alpha\beta\gamma}^G * \Delta u_\alpha n_\beta ds, \quad \mathbf{x} \notin \Gamma_c^+, \tag{9}$$

where $\sigma_{\alpha\beta\gamma}^G$ is the time-domain stress Green's functions, $\Delta u_\alpha(\mathbf{y},\tau)$ are the crack-opening-displacements (CODs) defined by

$$\Delta u_\alpha(\mathbf{y},\tau) = u_\alpha(\mathbf{y} \in \Gamma_c^+, \tau) - u_\alpha(\mathbf{y} \in \Gamma_c^-, \tau), \tag{10}$$

and an $*$ stands for Riemann convolution which is defined by

$$g(\mathbf{x},t) * h(\mathbf{x},t) = \int_0^t g(\mathbf{x},t-\tau)h(\mathbf{x},\tau)d\tau. \tag{11}$$

The stress Green's functions $\sigma_{\alpha\beta\gamma}^G$ are related to the displacement Green's functions $u_{\alpha\gamma}^G$ by Hooke's law (2), i.e.,

$$\begin{Bmatrix} \sigma_{11\gamma}^G \\ \sigma_{22\gamma}^G \\ \sigma_{12\gamma}^G \end{Bmatrix} = \begin{bmatrix} C_{11} & C_{12} & 0 \\ C_{21} & C_{22} & 0 \\ 0 & 0 & C_{66} \end{bmatrix} \begin{Bmatrix} u_{1\gamma,1}^G \\ u_{2\gamma,2}^G \\ u_{1\gamma,2}^G + u_{2\gamma,1}^G \end{Bmatrix}. \tag{12}$$

Substituting Eq. (9) into Hooke's law (2), taking the limit process $\mathbf{x} \to \Gamma_c^+$ and considering the traction boundary conditions (4), time-domain traction BIEs are obtained as

$$n_\beta(\mathbf{x}) \int_{\Gamma_c^+} T_{\gamma\alpha\beta}^G(\mathbf{x},\mathbf{y};t,\tau) * \Delta u_\gamma(\mathbf{y},\tau)ds = f_\alpha(\mathbf{x},t), \quad \mathbf{x} \in \Gamma_c^+, \tag{13}$$

where $T_{\gamma\alpha\beta}^G$ are time-domain traction Green's functions

which are related to the stress Green's functions $\sigma_{\gamma\alpha\beta}^G$ by

$$
\left\{ \begin{array}{c} T_{\gamma 11}^G \\ T_{\gamma 22}^G \\ T_{\gamma 12}^G \end{array} \right\} = - \left[\begin{array}{ccc} C_{11} & C_{12} & 0 \\ C_{21} & C_{22} & 0 \\ 0 & 0 & C_{66} \end{array} \right] \times
$$
$$
\left\{ \begin{array}{c} \sigma_{\gamma\alpha 1,1}^G n_\alpha \\ \sigma_{\gamma\alpha 2,2}^G n_\alpha \\ \left(\sigma_{\gamma\alpha 1,2}^G + \sigma_{\gamma\alpha 2,1}^G \right) n_\alpha \end{array} \right\}, \quad (14)
$$

The time-domain traction BIEs (13) are hypersingular, since $T_{\gamma\alpha\beta}^G(\mathbf{x},\mathbf{y};t,\tau)$ have the same singularity as their corresponding static Green's functions (see Wang and Achenbach, 1992, 1993, 1994, 1995), i.e.,

$$
T_{\gamma\alpha\beta}^G(\mathbf{x},\mathbf{y};t,\tau) \propto \frac{1}{|\mathbf{x}-\mathbf{y}|^2}, \qquad \text{for} \quad \mathbf{x} \to \mathbf{y}. \quad (15)
$$

The hypersingular integrals in (13) are undestood in the sense of Hadamard finite-part integrals. To solve the hypersingular traction BIEs (13), different methods, such as the Galerkin method, the regularization method and the direct method can be applied. This analysis uses a Galerkin method for spatial discretization and the convolution quadrature formula of Lubich (see e.g. Lubich, 1988a, 1988b, 1994; Lubich and Schneider, 1992) for temporal discretization of the time-domain traction BIEs (13). In this method, an explicit expression of the time-domain Green's functions $T_{\gamma\alpha\beta}^G(\mathbf{x},\mathbf{y};t,\tau)$ are not needed, and only their Laplace transform $\hat{T}_{\gamma\alpha\beta}^G(\mathbf{x},\mathbf{y};p)$ are required as will be seen in the next section.

3 Time-Stepping Scheme

This section presents a time-stepping scheme for solving the hypersingular time-domain traction BIEs (13). Here, the convolution quadrature formula of Lubich (see e.g. Lubich, 1988a, 1988b, 1994; Lubich and Schneider, 1992) is used for evaluating the temporal convolution while a Galerkin method is applied for the spatial approximation of the unknown CODs arising in the time-domain BIEs (13).

The unknown CODs $\Delta u_\gamma(y_1,\tau)$ are expanded into an infinite series of the form

$$
\Delta u_\gamma(y_1,\tau) = \sqrt{a^2 - y_1^2} \sum_{k=1}^{\infty} c_{\gamma;k}(\tau) U_{k-1}(y_1/a), \quad (16)
$$

where $c_{\gamma;k}(\tau)$ are unknown time-dependent expansion coefficients and $U_{k-1}(y_1/a)$ are Chebyshev polynomials of

second kind. Substituting Eq. (16) into Eq. (13), multiplying both sides by $\sqrt{a^2 - x_1^2} U_{l-1}(x_1/a)$, and integrating with respect to x_1 from $-a$ to $+a$, the following time-domain Galerkin traction BIEs are obtained

$$
\sum_{k=1}^{\infty} \int_{-a}^{+a} \sqrt{a^2 - x_1^2} U_{l-1}(x_1/a) \int_{-a}^{+a} \sqrt{a^2 - y_1^2} U_{k-1}(y_1/a) \times
$$
$$
T_{\gamma\alpha 2}^G(x_1,y_1;t,\tau) * c_{\gamma;k}(\tau) dy_1 dx_1 \quad (17)
$$
$$
= \int_{-a}^{+a} f_\alpha(x_1,t) \sqrt{a^2 - x_1^2} U_{l-1}(x_1/a) dx_1, \quad l = 1,2,...,\infty.
$$

By applying the convolution quadrature formula of Lubich (see e.g. Lubich, 1988a, 1988b, 1994; Lubich and Schneider, 1992)

$$
f(t) = g(t) * h(t) = \int_0^t g(t-\tau)h(\tau)d\tau
$$
$$
\implies f(n\Delta t) = \sum_{j=0}^{n} \omega_{n-j}(\Delta t) h(j\Delta t), \quad (18)
$$

to Eq. (17) a system of linear algebraic equations for the expanssion coefficients is obtained as

$$
\sum_{j=0}^{n} \sum_{k=1}^{\infty} A_{\gamma\alpha;kl}^{n-j} c_{\gamma;k}^j = f_{\alpha;l}^n, \quad (19)
$$
$$
(n = 0,1,...,N; \quad l = 1,2,...,\infty),
$$

where the time-variable t is devided into N equal time-steps Δt, and the upper indices indicate the time-steps. The system matrix in Eq. (19) corresponds to the integration weights $\omega_{n-j}(\Delta t)$ of the convolution quadrature formula (18). The system matrix $A_{\gamma\alpha;kl}^{n-j}$ and the right-hand side $f_{\alpha;l}^n$ of Eq. (19) can be obtained by using

$$
A_{\gamma\alpha;kl}^{n-j} = \frac{r^{-(n-j)}}{M} \sum_{m=0}^{M-1} \hat{A}_{\gamma\alpha;kl}(p_m) e^{-2\pi i(n-j)m/M}, \quad (20)
$$

$$
f_{\alpha;l}^n = (-1)^{l+1} \int_{-a}^{+a} f_\alpha(x_1,n\Delta t) \sqrt{a^2 - x_1^2} U_{l-1}(x_1/a) dx_1
$$
$$
= (-1)^{l+1} f_\alpha^* \times \left\{ \begin{array}{ll} \frac{\pi a^2}{2}, & l = 1, \\ \\ 0, & l \neq 1. \end{array} \right. \quad (21)
$$

where

$$p_m = \frac{\delta(\zeta_m)}{\Delta t}; \quad \delta(\zeta_m) = \sum_{j=1}^{2} \frac{(1-\zeta_m)^j}{j}; \quad \zeta_m = re^{2\pi i \cdot m/M}.$$

(22)

Here $M = N$ and $r^N = \sqrt{\varepsilon}$ are chosen with ε being the numerical error arised in the computation of the Laplace-transform of the system matrix $\hat{A}_{\gamma\alpha;kl}(p_m)$. ¿From Eq. (17) it follows that the Laplace-transform of the system matrix $\hat{A}_{\gamma\alpha;kl}(p_m)$ has the following form

$$\hat{A}_{\gamma\alpha;kl}(p_m) = (-1)^l n_\beta \int_{-a}^{+a} \sqrt{a^2 - x_1^2} U_{l-1}(x_1/a) \times$$

(23)

$$\int_{-a}^{+a} \hat{T}_{\gamma\alpha\beta}^G(x_1, y_1; p_m) \sqrt{a^2 - y_1^2} U_{k-1}(y_1/a) dy_1 dx_1.$$

in which $\hat{T}_{\gamma\alpha\beta}^G(x_1, y_1; p)$ represents Green's functions in the Laplace transform domain. The numerical computation of the system matrix in the Laplace-domian $\hat{A}_{\gamma\alpha;kl}(p_m)$ will be explained in the next section.

Unlike the conventional time-domain BIE formulation which uses in general very complicated time-domain Green's functions, the present time-domain BIEM applies Laplace-domain Green's functions. Thus, the present method requires no explicit expression of the time-domain Green's functions $T_{\gamma\alpha\beta}^G$. The Laplace-domain Green's functions $\hat{T}_{\gamma\alpha\beta}^G$ needed here are expressed as Fourier integrals as will be shown in the next section. The system matrix defined by Eq. (20) is symmetric, real-valued and it is the real-part of the right-hand side of Eq. (20). The evaluation of Eq. (20) can be performed very efficiently by using the Fast Fourier Transform (FFT).

By considering the zero initial conditions (3), the following time-stepping scheme is obtained from the system of linear algebraic equations (19)

$$c_{\gamma;k}^n = \sum_{l=1}^{\infty} \left(A_{\gamma\alpha;kl}^0\right)^{-1} \left[f_{\alpha;l}^n - \sum_{j=1}^{n-1} \sum_{i=1}^{\infty} A_{\beta\alpha;li}^{n-j} c_{\beta;i}^j \right],$$

$$(n = 1, 2, ..., N), \quad (24)$$

in which $(A_{\gamma\alpha;kl}^0)^{-1}$ represents the inverse matrix of $A_{\gamma\alpha;kl}^0$ at the time-step $n=0$. Eq. (24) can be used to obtain the expansion coefficients $c_{\gamma;k}^n$ time-step by time-step. The elastodynamic stress intensity factors can be computed immediately from the numerically calculated CODs.

4 Computation of the System Matrix in Laplace-Domain

To compute the system matrix in the Laplace-domain $\hat{A}_{\gamma\alpha;kl}(p_m)$, the generic boundary value problem in the Laplace transform domain is described in this section. Applying the one-sided Laplace transform defined by

$$\hat{f}(p) = \int_{0}^{\infty} f(t)e^{-pt}dt; \qquad f(t) = \frac{1}{2\pi i}\int_{Br} \hat{f}(p)e^{pt}dp;$$

(25)

to Eq. (1) the equations of motion can be written as

$$\hat{\sigma}_{\alpha\beta,\beta} = \rho p^2 \hat{u}_\alpha,$$

(26)

where p in Eq. (25) is a transform parameter and Br denotes the Bromwich integration path which is a line to the right-hand side and parallel to the imaginary axis in the complex p-plane. The boundary and the continuity conditions on the crack-faces $|x_1| \leq a$ and the crack-plane $|x_1| \leq \infty$ can be stated as

$$\hat{\sigma}_{\alpha 2}(x_1, 0) = \hat{f}_\alpha(x_1, 0), \qquad |x_1| \leq a.$$

(27)

$$\hat{\sigma}_{\alpha 2}(x_1, 0^+) = \hat{\sigma}_{\alpha 2}(x_1, 0^-), \qquad |x_1| < \infty,$$

(28)

$$\hat{u}_\alpha(x_1, 0^+) = \hat{u}_\alpha(x_1, 0^-), \qquad |x_1| \geq a.$$

(29)

Across the crack-faces, the displacements jump, i.e.,

$$\hat{u}_\alpha(x_1, 0^+) - \hat{u}_\alpha(x_1, 0^-) = \Delta\hat{u}_\alpha(x_1), \qquad |x_1| < a, \quad (30)$$

where $\Delta\hat{u}_\alpha(x_1)$ are the crack-opening-displacements in the Laplace transform domain.

The displacements $\hat{u}_\gamma$ are expressed as the following Fourier integrals

$$\hat{u}_\gamma(\mathbf{x}) = \begin{cases} \int_{-\infty}^{\infty} \sum_{\beta=1}^{2} B_\gamma^\beta(\xi) \exp(i\xi x_1 - \gamma_\beta x_2) d\xi, & x_2 > 0, \\ \int_{-\infty}^{\infty} \sum_{\beta=1}^{2} D_\gamma^\beta(\xi) \exp(i\xi x_1 + \gamma_\beta x_2) d\xi, & x_2 < 0. \end{cases}$$

(31)

Substitution of Eq. (31) into Hooke's law (2) and subsequently into euqations of motion (26) results in the following relations

$$B_2^\beta = \lambda_\beta B_1^\beta; \qquad D_2^\beta = -\lambda_\beta D_1^\beta; \qquad \text{(no sum over } \beta\text{)},$$

(32)

and the characteristic equation for γ_β

$$a\gamma_\beta^4 + b\gamma_\beta^2 + c = 0, \tag{33}$$

where

$$\lambda_\beta = \frac{1}{(C_{12}+C_{66})(i\xi)\gamma_\beta}\left(C_{66}\gamma_\beta^2 - C_{11}\xi^2 - \rho p^2\right);$$

$$a = \frac{C_{22}}{C_{66}};$$

$$b = -\left\{\left(\frac{C_{22}}{C_{66}}+1\right)\frac{\rho}{C_{66}}p^2 + \left[\frac{C_{11}}{C_{66}}\cdot\frac{C_{22}}{C_{66}} - \left(\frac{C_{12}}{C_{66}}\right)^2\right.\right.$$

$$\left.\left. -2\frac{C_{12}}{C_{66}}\right]\xi^2\right\};$$

$$c = \left(\frac{C_{11}}{C_{66}}\xi^2 + \frac{\rho}{C_{66}}p^2\right)\left(\xi^2 + \frac{\rho}{C_{66}}p^2\right). \tag{34}$$

Eq. (33) has the simple solutions

$$\gamma_\beta^2 = \frac{1}{2a}\left(-b + (-1)^{\beta-1}\sqrt{b^2 - 4ac}\right). \tag{35}$$

In Eq. (31), $Re(\gamma_\beta) \geq 0$ due to the radiation conditions at infinity, and $B_\gamma^\beta(\xi)$ and $D_\gamma^\beta(\xi)$ are unknown functions which have to be determined.

Stress components are obtained by substituting Eq. (31) into Hokke's law (2) as

$$\left\{\begin{array}{c}\hat{\sigma}_{11}\\\hat{\sigma}_{22}\\\hat{\sigma}_{12}\end{array}\right\} = \left[\begin{array}{ccc}C_{11} & C_{12} & 0\\C_{21} & C_{22} & 0\\0 & 0 & C_{66}\end{array}\right] \times$$

$$\left\{\begin{array}{c}\int_{-\infty}^{\infty}\sum_{\beta=1}^{2}B_1^\beta(i\xi)\exp(i\xi x_1 - \gamma_\beta x_2)d\xi\\\int_{-\infty}^{\infty}\sum_{\beta=1}^{2}B_2^\beta(-\gamma_\beta)\exp(i\xi x_1 - \gamma_\beta x_2)d\xi\\\int_{-\infty}^{\infty}\sum_{\beta=1}^{2}[B_1^\beta(-\gamma_\beta) + B_2^\beta(i\xi)]\exp(i\xi x_1 - \gamma_\beta x_2)d\xi\end{array}\right\},$$

$$x_2 > 0, \tag{36}$$

$$\left\{\begin{array}{c}\hat{\sigma}_{11}\\\hat{\sigma}_{22}\\\hat{\sigma}_{12}\end{array}\right\} = \left[\begin{array}{ccc}C_{11} & C_{12} & 0\\C_{21} & C_{22} & 0\\0 & 0 & C_{66}\end{array}\right] \times$$

$$\left\{\begin{array}{c}\int_{-\infty}^{\infty}\sum_{\beta=1}^{2}D_1^\beta(i\xi)\exp(i\xi x_1 + \gamma_\beta x_2)d\xi\\\int_{-\infty}^{\infty}\sum_{\beta=1}^{2}D_2^\beta\gamma_\beta\exp(i\xi x_1 + \gamma_\beta x_2)d\xi\\\int_{-\infty}^{\infty}\sum_{\beta=1}^{2}[D_1^\beta\gamma_\beta + D_2^\beta(i\xi)]\exp(i\xi x_1 + \gamma_\beta x_2)d\xi\end{array}\right\},$$

$$x_2 < 0, \tag{37}$$

By substituting Eqs. (36) and (37) into the stress continuity equations (28) the following relations are obtained

$$\sum_{\beta=1}^{2}\left[-\gamma_\beta B_1^\beta + (i\xi)B_2^\beta - \gamma_\beta D_1^\beta - (i\xi)D_2^\beta\right] = 0, \tag{38}$$

$$\sum_{\beta=1}^{2}\left[C_{12}(i\xi)B_1^\beta - C_{22}\gamma_\beta B_2^\beta - C_{12}(i\xi)D_1^\beta - C_{22}\gamma_\beta D_2^\beta\right] = 0. \tag{39}$$

Substitution of Eq. (31) into the displacement continuity and discontinuity equations (29) and (30) leads to

$$\int_{-\infty}^{\infty}\sum_{\beta=1}^{2}(B_\gamma^\beta - D_\gamma^\beta)\exp(i\xi x_1)d\xi = \left\{\begin{array}{ll}0, & |x_1| > a,\\\Delta\hat{u}_\gamma(x_1), & |x_1| < a.\end{array}\right. \tag{40}$$

Eq. (40) can be inverted as

$$\sum_{\beta=1}^{2}(B_\gamma^\beta - D_\gamma^\beta) = \frac{1}{2\pi}\int_{-a}^{+a}\Delta\hat{u}_\gamma(y_1)\exp(-i\xi y_1)dy_1. \tag{41}$$

Eqs. (38), (39) and (41) together with Eq. (32) result in four algebraic equations for the four unknown functions B_1^β und D_1^β

$$\left[\begin{array}{cccc}a_1 & a_2 & a_1 & a_2\\b_1 & b_2 & -b_1 & -b_2\\1 & 1 & -1 & -1\\\lambda_1 & \lambda_2 & \lambda_1 & \lambda_2\end{array}\right]\left\{\begin{array}{c}B_1^1\\B_1^2\\D_1^1\\D_1^2\end{array}\right\} = \left\{\begin{array}{c}0\\0\\d_1\\d_2\end{array}\right\}, \tag{42}$$

where

$$a_\alpha = (i\xi)\lambda_\alpha - \gamma_\alpha; \quad b_\alpha = C_{12}(i\xi) - C_{22}\gamma_\alpha\lambda_\alpha;$$

$$\text{(no sum over } \alpha), \tag{43}$$

$$d_\alpha = \frac{1}{2\pi}\int_{-a}^{+a}\Delta\hat{u}_\alpha(y_1)\exp(-i\xi y_1)dy_1. \tag{44}$$

Eqs. (42) have the following solutions

$$B_1^1 = \frac{1}{2}\left(\frac{b_2}{b_2-b_1}d_1 + \frac{a_2}{a_2\lambda_1 - a_1\lambda_2}d_2\right), \tag{45}$$

$$B_1^2 = -\frac{1}{2}\left(\frac{b_1}{b_2-b_1}d_1 + \frac{a_1}{a_2\lambda_1 - a_1\lambda_2}d_2\right), \tag{46}$$

$$D_1^1 = \frac{1}{2}\left(\frac{-b_2}{b_2 - b_1}d_1 + \frac{a_2}{a_2\lambda_1 - a_1\lambda_2}d_2\right), \qquad (47)$$

$$D_1^2 = \frac{1}{2}\left(\frac{b_1}{b_2 - b_1}d_1 - \frac{a_1}{a_2\lambda_1 - a_1\lambda_2}d_2\right). \qquad (48)$$

By substituting Eqs. (32) and (44)-(48) into Eq. (31) an expression for $\hat{u}_\gamma(\mathbf{x})$ is obtained as

$$\hat{u}_\gamma(\mathbf{x}) = \int_{-a}^{+a} \hat{\sigma}_{\alpha 2\gamma}^G(\mathbf{x},\mathbf{y};p)\Delta\hat{u}_\alpha(y_1)dy_1, \qquad (49)$$

where the stress Green's functions $\hat{\sigma}_{\alpha 2\gamma}^G(\mathbf{x},\mathbf{y};p)$ are given by

$$\hat{\sigma}_{\alpha 2\gamma}^G(\mathbf{x},\mathbf{y};p) = \frac{1}{4\pi} \times$$
$$\int_{-\infty}^{\infty}\sum_{\beta=1}^{2} S_{\alpha\gamma}^\beta \exp[i\xi(x_1 - y_1) - \gamma_\beta|x_2 - y_2|]d\xi, \quad (50)$$

in which

$$S_{11}^1 = \frac{b_2}{b_2 - b_1}sgn; \quad S_{11}^2 = \frac{-b_1}{b_2 - b_1}sgn;$$

$$S_{21}^1 = \frac{a_2}{a_2\lambda_1 - a_1\lambda_2}; \quad S_{21}^2 = \frac{-a_1}{a_2\lambda_1 - a_1\lambda_2};$$

$$S_{12}^1 = \frac{b_2\lambda_1}{b_2 - b_1}; \quad S_{12}^2 = \frac{-b_1\lambda_2}{b_2 - b_1};$$

$$S_{22}^1 = \frac{a_2\lambda_1}{a_2\lambda_1 - a_1\lambda_2}sgn; \quad S_{22}^2 = \frac{-a_1\lambda_2}{a_2\lambda_1 - a_1\lambda_2}sgn;$$

$$sgn = \begin{cases} +1, & x_2 > y_2, \\ -1, & x_2 < y_2. \end{cases} \qquad (51)$$

By the same way, substitution of Eqs. (32) and (44)-(48) into Eqs. (36) and (37) yields a representation integral for the stress components $\hat{\sigma}_{\alpha\delta}(\mathbf{x})$

$$\hat{\sigma}_{\alpha\delta}(\mathbf{x}) = \int_{-a}^{+a} \hat{T}_{\gamma\alpha\delta}^G(x_1,y_1;p)\Delta\hat{u}_\gamma(y_1)dy_1, \qquad (52)$$

in which the traction Green's functions $\hat{T}_{\gamma\alpha\delta}^G(\mathbf{x},\mathbf{y};p)$ are given by

$$\hat{T}_{\gamma\alpha\delta}^G(\mathbf{x},\mathbf{y};p) = -\frac{1}{4\pi} \times$$
$$\int_{-\infty}^{\infty}\sum_{\beta=1}^{2} \overline{T}_{\gamma\alpha\delta}^\beta \exp[i\xi(x_1 - y_1) - \gamma_\beta|x_2 - y_2|]d\xi, \quad (53)$$

where $\overline{T}_{\gamma\alpha\delta}^\beta = \overline{T}_{\gamma\delta\alpha}^\beta$, and

$$\overline{T}_{111}^1 = \frac{b_2c_1}{b_2 - b_1}sgn; \quad \overline{T}_{111}^2 = \frac{-b_1c_2}{b_2 - b_1}sgn;$$

$$\overline{T}_{211}^1 = \frac{a_2c_1}{a_2\lambda_1 - a_1\lambda_2}; \quad \overline{T}_{211}^2 = \frac{-a_1c_2}{a_2\lambda_1 - a_1\lambda_2};$$

$$\overline{T}_{112}^1 = C_{66}\frac{a_1b_2}{b_2 - b_1}; \quad \overline{T}_{112}^2 = C_{66}\frac{-a_2b_1}{b_2 - b_1};$$

$$\overline{T}_{212}^1 = C_{66}\frac{a_1a_2}{a_2\lambda_1 - a_1\lambda_2}sgn; \quad \overline{T}_{212}^2 = -\overline{T}_{212}^1;$$

$$\overline{T}_{122}^1 = \frac{b_1b_2}{b_2 - b_1}sgn; \quad \overline{T}_{122}^2 = -\overline{T}_{122}^1;$$

$$\overline{T}_{222}^1 = \frac{a_2b_1}{a_2\lambda_1 - a_1\lambda_2}; \quad \overline{T}_{222}^2 = \frac{-a_1b_2}{a_2\lambda_1 - a_1\lambda_2};$$

$$c_\alpha = C_{11}(i\xi) - C_{12}\gamma_\alpha\lambda_\alpha; \quad \text{(no sum over } \alpha\text{)}. \qquad (54)$$

Substituting Eq. (53) into Eq. (23) and using the relations

$$\int_{-1}^{1} \sqrt{1-\eta^2}U_{k-1}(\eta)\exp(i\alpha\eta)d\eta =$$
$$\frac{k\pi}{\alpha}J_k(\alpha)\exp\left[i(k-1)\frac{\pi}{2}\right], \quad (55)$$

$$a_1b_2 - a_2b_1 = \frac{i(\gamma_1 - \gamma_2)}{(C_{11} + C_{66})\gamma_1\gamma_2\xi} \times$$
$$[(C_{11}\xi^2 + \rho p^2)(C_{22}\gamma_1\gamma_2 + \rho p^2) - C_{12}^2\gamma_1\gamma_2\xi^2] \quad (56)$$

$$b_2 - b_1 = -\frac{iC_{22}C_{66}}{(C_{12} + C_{66})\xi}(\gamma_1^2 - \gamma_2^2), \qquad (57)$$

$$a_2\lambda_1 - a_1\lambda_2 = \frac{i(\gamma_1^2 - \gamma_2^2)}{(C_{11} + C_{66})\gamma_1\gamma_2\xi}(C_{11}\xi^2 + \rho p^2), \qquad (58)$$

the system matrix in the Laplace-domain $\hat{A}_{\gamma\alpha;kl}(p_m)$ can be evaluated as

$$\hat{A}_{\gamma\alpha;kl}(p_m) = -\frac{\pi}{4}(-1)^l(kl)a^2 C_{66}\int_0^{\infty} F_{\gamma\alpha}(\xi, p_m)\frac{1}{\xi^2} \times$$
$$J_k(-\xi a)J_l(\xi a)\exp\left[3i(k+l)\frac{\pi}{2}\right]d\xi, \quad (59)$$

where $J_k(\cdot)$ is the Bessel function of first kind and k-th order, and

$$F_{\gamma\alpha} = \begin{bmatrix} \dfrac{\overline{F}}{(C_{22}/C_{66})\gamma_1\gamma_2} & 0 \\ 0 & \dfrac{\overline{F}}{(C_{11}/C_{66})\xi^2 + (\rho/C_{66})p_m^2} \end{bmatrix},$$

(60)

in which

$$
\overline{F} = \frac{1}{\gamma_1 + \gamma_2}\left[\left(\frac{C_{11}}{C_{66}}\xi^2 + \frac{\rho}{C_{66}}p_m^2\right)\left(\frac{C_{22}}{C_{66}}\gamma_1\gamma_2 + \frac{\rho}{C_{66}}p_m^2\right)\right.
$$
$$
\left. - \left(\frac{C_{12}}{C_{66}}\right)^2\gamma_1\gamma_2\xi^2\right]. \tag{61}
$$

By invoking the relation (Abramowitz and Stegun, 1972)

$$
J_k(-z) = (-1)^k J_k(z), \qquad (k \quad \text{integer}), \tag{62}
$$

Eq. (59) can be rewritten as

$$
\hat{A}_{\gamma\alpha;kl}(p_m) = \begin{cases} 0, & k+l \quad \text{odd}, \\[2mm] -\dfrac{\pi}{2}(kl)a^2 i^{k+l}C_{66}\displaystyle\int_0^\infty F_{\gamma\alpha}(\xi, p_m)\dfrac{1}{\xi^2} \times \\[2mm] \quad J_k(\xi a)J_l(\xi a)d\xi, & k+l \quad \text{even}. \end{cases}
$$
$$\tag{63}$$

For $\xi \to \infty$, the integrand in Eq. (63) behaves as $1/\xi^2$ due to the following asymptotics of the Bessel function (Abramowitz and Stegun, 1972)

$$
J_k(z) \sim \sqrt{\frac{2}{\pi z}}, \qquad |z| \to \infty, \quad |z| \geq |k|, \tag{64}
$$

and the asymptotic behavior

$$
F_{\gamma\alpha}(\xi, p_m)\frac{1}{\xi^2} = G_{\gamma\alpha}\cdot\frac{1}{\xi}, \qquad \xi \to \infty, \tag{65}
$$

in which

$$
G_{11} = \frac{1}{(C_{22}/C_{66})(H_1 + H_2)}\left[\frac{C_{11}}{C_{66}}\cdot\frac{C_{22}}{C_{66}} - \left(\frac{C_{12}}{C_{66}}\right)^2\right];
$$
$$
G_{22} = \frac{H_1 H_2}{(C_{11}/C_{66})(H_1 + H_2)}\left[\frac{C_{11}}{C_{66}}\cdot\frac{C_{22}}{C_{66}} - \left(\frac{C_{12}}{C_{66}}\right)^2\right];
$$
$$
G_{12} = G_{21} = 0;
$$
$$
H_{1,2}^2 = \frac{1}{2(C_{22}/C_{66})}\left\{\left[\frac{C_{11}}{C_{66}}\cdot\frac{C_{22}}{C_{66}} - \left(\frac{C_{12}}{C_{66}}\right)^2 - 2\frac{C_{12}}{C_{66}}\right] \pm \right.
$$
$$
\left. \sqrt{\left[\frac{C_{11}}{C_{66}}\cdot\frac{C_{22}}{C_{66}} - \left(\frac{C_{12}}{C_{66}}\right)^2 - 2\frac{C_{12}}{C_{66}}\right]^2 - 4\frac{C_{11}}{C_{66}}\cdot\frac{C_{22}}{C_{66}}}\right\} \tag{66}
$$

The slow convergency rate $1/\xi^2$ of the integrand in Eq. (63) is inconvenient for numerically computing the system matrix in the Laplace-domain. To get a better convergency, Eq. (63) is recast into

$$
\hat{A}_{\gamma\alpha;kl}(p_m) = -\frac{\pi}{2}(kl)a^2 i^{k+l}C_{66}\left\{\int_0^\infty\left[F_{\gamma\alpha}(\xi, p_m)\frac{1}{\xi^2} - G_{\gamma\alpha}\cdot\frac{1}{\xi}\right] \times \right.
$$
$$
\left. J_k(\xi a)J_l(\xi a)d\xi + G_{\gamma\alpha}\frac{\delta_{kl}}{k+l}\right\}, \quad k+l \quad \text{even}, \tag{67}
$$

where use is made of the orthogonality relation of the Bessel function (Abramowitz and Stegun, 1972)

$$
\int_0^\infty \frac{1}{z}J_k(z)J_l(z)dz = \frac{\delta_{kl}}{k+l}. \tag{68}
$$

It can be easily shown that for $\xi \to \infty$ the integrand in Eq. (67) behaves as $1/\xi^4$, and the infinite integral of Eq. (67) thus converges much more faster than the corresponding integral of Eq. (63) does. For the numerical computation of the system matrix in the Laplace-domain $\hat{A}_{\gamma\alpha;kl}(p_m)$, the fast convergence of the infinite integral in (67) is very advantageous.

The system matrix $\hat{A}_{\gamma\alpha;kl}(p_m)$ is symmetric, complex-valued and has to be computed at N discrete values p_m ($m = 0, 1, 2, ...N - 1$). Subsequently, the system matrix $A^n_{\gamma\alpha;kl}$ ($n = 0, 1, 2, ..., N$) at $N+1$ time-steps can be evaluated by using Eq. (20). Note here that the present method requires only a numerical integration of a single integral, while the usual Galerkin method in general involves a numerical integration of triple integrals in anisotropic cases, since the Laplace-domain Green's functions do not have closed form expressions. Here, the triple integrals arising in the system matrix are evaluated analytically twice which makes the numerical scheme especially efficient and attractive. The infinite integral of (67) is computed numerically by using an adaptive Romberg quadrature method in conjunction with the truncation method. The upper limit of the integration in the truncation method is taken as $\xi a = 20$ which is sufficient.

5 Computation of Elastodynamic Stress Intensity Factors

At a crack-tip in linear elastic and anisotropic solids, the displacement field has the following asymptotic expres-

sions

$$u_1 = \sqrt{\frac{2r}{\pi}} \left\{ K_I Re \left[\frac{1}{\mu_1 - \mu_2} \left(\mu_1 p_2 \sqrt{\cos\theta + \mu_2 \sin\theta} \right. \right. \right.$$
$$\left. \left. \left. - \mu_2 p_1 \sqrt{\cos\theta + \mu_1 \sin\theta} \right) \right] \right.$$
$$\left. + K_{II} Re \left[\frac{1}{\mu_1 - \mu_2} \left(p_2 \sqrt{\cos\theta + \mu_2 \sin\theta} \right. \right. \right.$$
$$\left. \left. \left. - p_1 \sqrt{\cos\theta + \mu_1 \sin\theta} \right) \right] \right\}, \quad (69)$$

$$u_2 = \sqrt{\frac{2r}{\pi}} \left\{ K_I Re \left[\frac{1}{\mu_1 - \mu_2} \left(\mu_1 q_2 \sqrt{\cos\theta + \mu_2 \sin\theta} \right. \right. \right.$$
$$\left. \left. \left. - \mu_2 q_1 \sqrt{\cos\theta + \mu_1 \sin\theta} \right) \right] \right.$$
$$\left. + K_{II} Re \left[\frac{1}{\mu_1 - \mu_2} \left(q_2 \sqrt{\cos\theta + \mu_2 \sin\theta} \right. \right. \right.$$
$$\left. \left. \left. - q_1 \sqrt{\cos\theta + \mu_1 \sin\theta} \right) \right] \right\}, \quad (70)$$

where K_I and K_{II} are the mode-I and mode-II stress intensity factors, r and θ are polar coordinates with the origin centered at the crack-tip, μ_α are the complex roots of the material characteristic equation

$$b_{11}\mu^4 + (2b_{12} + b_{66})\mu^2 + b_{22} = 0, \quad (71)$$

b_{ij} $(i, j = 1, 2, 6)$ is the material compliance matrix, and

$$p_\alpha = b_{11}\mu_\alpha^2 + b_{12}; \quad q_\alpha = b_{12}\mu_\alpha + b_{22}/\mu_\alpha. \quad (72)$$

For orthotropic solids, the material compliance matrix b_{ij} is related to the engineering elastic constants by

$$\begin{bmatrix} \frac{1}{E_1} & -\frac{\nu_{12}}{E_1} & 0 \\ -\frac{\nu_{21}}{E_2} & \frac{1}{E_2} & 0 \\ 0 & 0 & \frac{1}{G_{12}} \end{bmatrix} \quad (73)$$

for generalized plane stress, and

$$\begin{bmatrix} \frac{1}{E_1} - \frac{\nu_{21}^2}{E_2} & -\frac{\nu_{12}}{E_1} - \frac{\nu_{12}\nu_{32}}{E_1} & 0 \\ -\frac{\nu_{21}}{E_2} - \frac{\nu_{21}\nu_{32}}{E_2} & \frac{1}{E_2} - \frac{\nu_{32}^2}{E_2} & 0 \\ 0 & 0 & \frac{1}{G_{12}} \end{bmatrix} \quad (74)$$

for generalized plane strain. The characteristic equation (71) has the solutions

$$\mu_1 = \sqrt{\frac{\alpha_0 - \beta_0}{2}} + i\sqrt{\frac{\alpha_0 + \beta_0}{2}},$$
$$\mu_2 = -\sqrt{\frac{\alpha_0 - \beta_0}{2}} + i\sqrt{\frac{\alpha_0 + \beta_0}{2}}, \quad (75)$$

in which

$$\alpha_0 = \sqrt{\frac{b_{22}}{b_{11}}}; \quad \beta_0 = \frac{2b_{12} + b_{66}}{2b_{11}}. \quad (76)$$

The asymptotic displacement field described by Eqs. (69) and (70) yields then the following relation between the elastodynamic stress intensity factors and the crack-opening-displacements

$$\left\{ \begin{array}{c} K_I^\pm(t) \\ K_{II}^\pm(t) \end{array} \right\} = \frac{\sqrt{2\pi}}{8\sqrt{(\alpha_0 + \beta_0)/2}} \lim_{x_1 \to \pm a} \frac{1}{\sqrt{a \mp x_1}} \times$$
$$\left\{ \begin{array}{c} \frac{\alpha_0}{b_{22}} \Delta u_2(x_1, t) \\ \frac{1}{b_{11}} \Delta u_1(x_1, t) \end{array} \right\}, \quad (77)$$

where "$\pm$" indicates the left and the right crack-tips at $x_1 = +a$ and $x_1 = -a$.

Substituting Eq. (16) into Eq. (77) and using the identity (Abramowitz and Stegun, 1972)

$$U_{k-1}(\pm 1) = (\pm 1)^{k-1} k \quad (78)$$

a relation between the elastodynamic stress intensity factors and the expansion coefficients $c_{\gamma;k}(t)$ is obtained as

$$\left\{ \begin{array}{c} K_I^\pm(t) \\ K_{II}^\pm(t) \end{array} \right\} = \frac{\sqrt{\pi a}}{4\sqrt{(\alpha_0 + \beta_0)/2}} \times$$
$$\left\{ \begin{array}{c} \frac{\alpha_0}{b_{22}} \sum_{k=1}^{\infty} (\pm 1)^{k-1} k c_{2;k}(t) \\ \frac{1}{b_{11}} \sum_{k=1}^{\infty} (\pm 1)^{k-1} k c_{1;k}(t) \end{array} \right\}. \quad (79)$$

Once the expansion coefficients $c_{\gamma;k}(t)$ have been determined numerically by using the time-stepping scheme (24), the elastodynamic stress intensity factors can be calculated by using Eq. (79).

For convenience, normalized elastodynamic stress intensity factors $\overline{K}_I^{\pm}$ and $\overline{K}_{II}^{\pm}$ are introduced as

$$\overline{K}_I^{\pm}(t) = K_I^{\pm}(t)/K_I^{st}; \qquad \overline{K}_{II}^{\pm}(t) = K_{II}^{\pm}(t)/K_{II}^{st}, \qquad (80)$$

where K_I^{st} and K_{II}^{st} are the corresponding static stress intensity factors of a finite crack of length $2a$ contained in an infinite orthotropic solid subjected to remote static stress loadings σ_{22}^{st} and σ_{12}^{st} at infinity, i.e.,

$$K_I^{st} = \sigma_{22}^{st}\sqrt{\pi a}; \qquad K_{II}^{st} = \sigma_{12}^{st}\sqrt{\pi a}. \qquad (81)$$

6 Numerical Examples

To test the accuracy and the stability of the present time-domain traction BIEM, a finite crack in an unbounded isotropic solid is first considered. The crack is subjected to an impact loading on the crack-faces as shown in Fig. 1. Numerical results for the normalized mode-I and mode-II elastodynamic stress intensity factors are shown in Fig. 2, versus the dimensionless time $c_L t/a$, where $c_L = \sqrt{(\lambda+\mu)/\rho}$ is the velocity of the longitudinal wave with λ and μ being the Lamé's elastic constants. In the numerical calculation, Poisson's ratio is taken as $\nu=0.25$, plane strain is assumed, 20 terms in the Galerkin-ansatz (16) for k and l are used, and the time-step is selected as $c_T t/a = 0.1$, with $c_T = \sqrt{\mu/\rho}$ being the velocity of the transverse shear wave. The parameters used in the computation of the time-dependent system matrix $A_{\gamma\alpha;kl}^n$ defined by Eq. (20) are chosen as: $M = N$, $\varepsilon = 10^{-12}$ and $r^N = \sqrt{\varepsilon}$. A comparison between the present numerical results and the analytical results of Thau and Lu (1971) as well as the numerical results of Zhang and Savaidis (1999) shows very good agreements, which confirms the high accuracy of the present time-domain traction BIEM. The analytical results of Thau and Lu (1971) were obtained by a Wiener-Hopf technique for solving the integral equations and they are valid only in the short-time range before the arrival of the diffracted waves from one crack-tip to the crack-tip considered. The numerical results of Zhang and Savaidis (1999) were obtained by a hypersingular time-domain traction BEM, where time-domain Green's functions were applied and the same time-step was used.

The effects of the upper truncation limits $K = L$ (number of terms of Chebyshev polynomials) for k and l, which are needed for computing the system matrix $A_{\gamma\alpha;kl}^n$, on the numerical results are shown in Fig. 3. The time-step used here is $c_T \Delta t = a/20$. By trial and error it is concluded
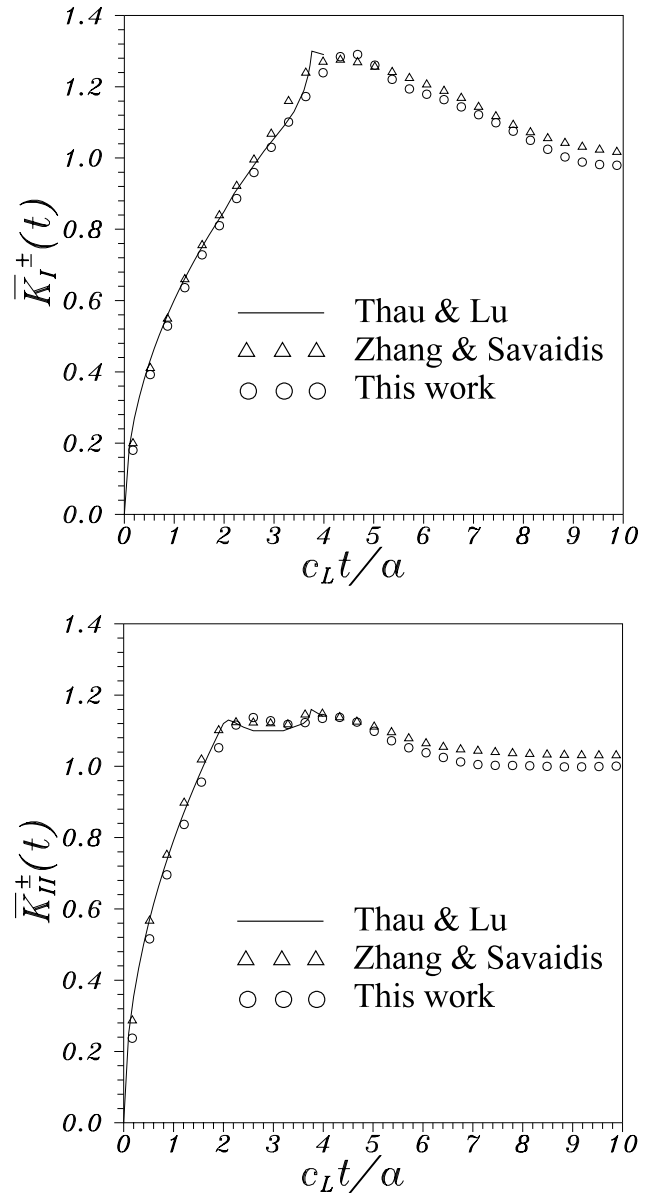

Figure 2 : Normalized $\overline{K}_I^{\pm}$- and $\overline{K}_{II}^{\pm}$-factors (isotropic solids)

that to keep the error of the numerically computed elastodynamic stress intensity factors less than 3% it is sufficient to take $K = L = 10$. Fig. 3 shows that no essential improvements can be obtained by using $K = L = 20$ and $K = L = 40$.

Fig. 4 shows the dependence of the numerical results on the choice of the time-step $c_T \Delta t$, where 40 terms of Chebyshev polynomials, i.e., $K = L = 40$ were used. Fig. 4 reveals that a time-step $c_T \Delta t = a/20$ is sufficient to ob-
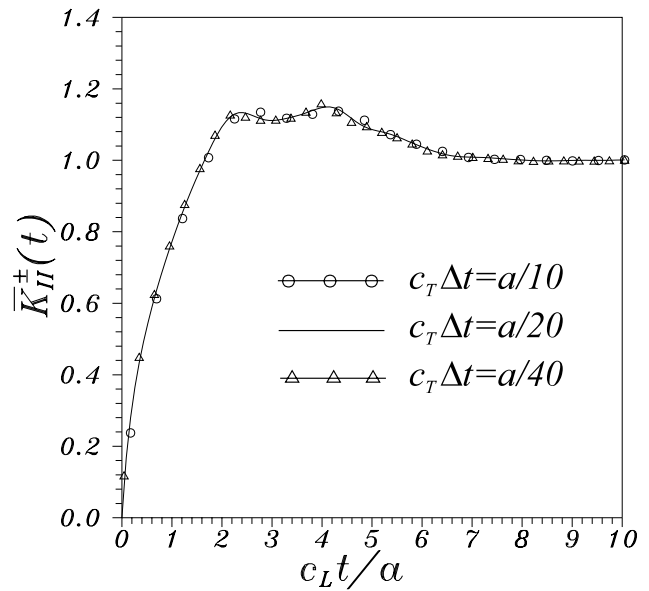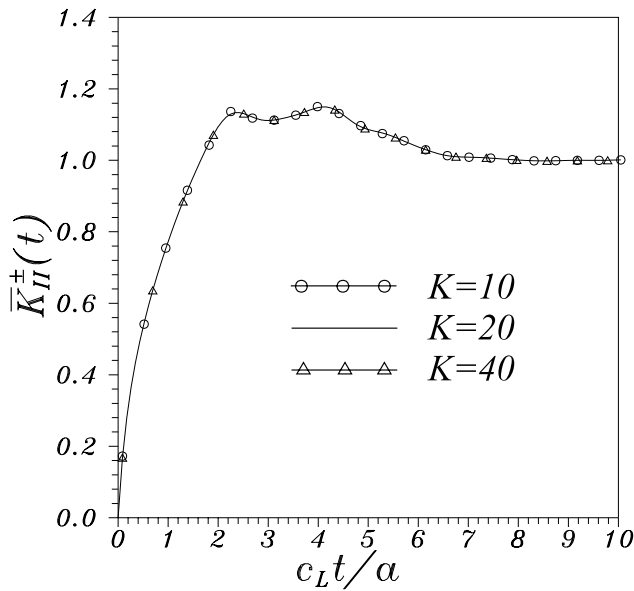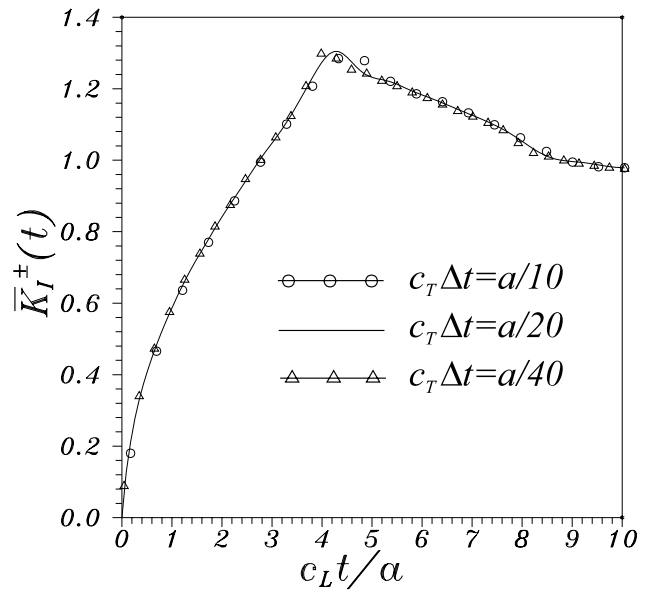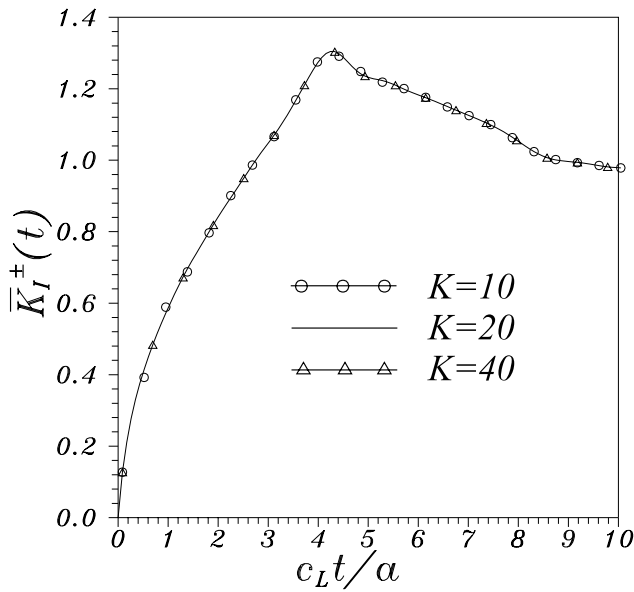
Figure 3 : Effects of the truncation limit K on $\overline{K}_I^{\pm}$- and $\overline{K}_{II}^{\pm}$-factors ($c_T \Delta t = a/20$, isotropic solids)

Figure 4 : Effects of the time-step $c_T \Delta t$ on $\overline{K}_I^{\pm}$- and $\overline{K}_{II}^{\pm}$-factors ($K = 40$, isotropic solids)

tain accurate numerical results, and a smaller time-step than $c_T \Delta t = a/20$ does not influence the numerical results significantly. Thus, all results presented below are obtained with a time-step $c_T \Delta t = a/20$. Furthermore, Fig. 4 shows that the present time-domain BIEM using the convolution quadrature of Lubich (1988a,1988b, 1994) is pretty insensitive to the choice of the time-step, in contrast to the conventional time-domain BEM using time-dependent Green's functions. In the time range con-

sidered in this analysis, the present time-domain traction BIEM provides stable numerical results for all the three time-steps $c_T \Delta t = a/10$, $a/20$ and $a/40$.

Next, a class of orthotropic materials investigated by Kassir and Bandyopadhyay (1983) is considered. The corresponding engineering elastic constants are listed in Tab. 1. Numerical results for the normalized mode-I and mode-II elastodynamic stress intensity factors are presented in Figs. (5)-(10) and compared with those ob-
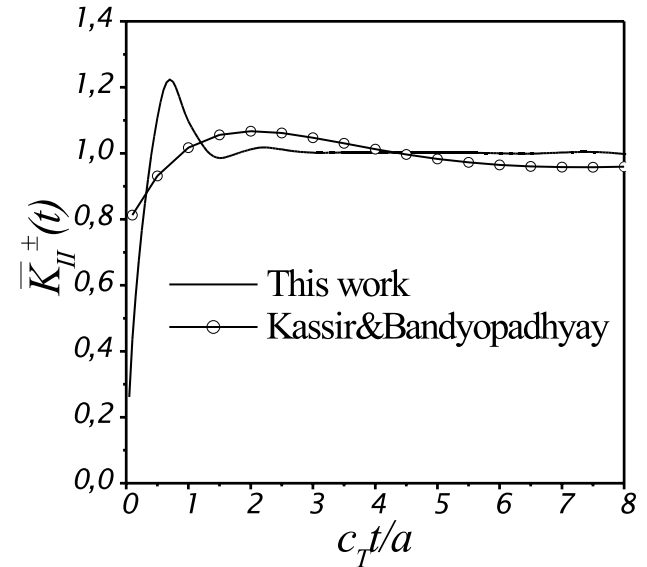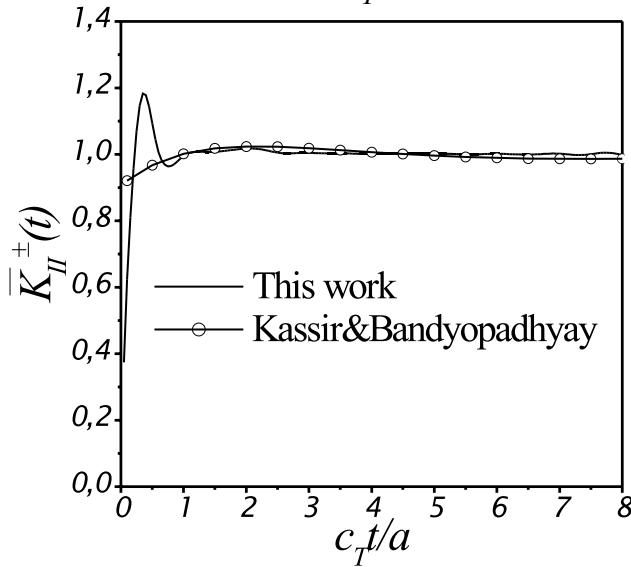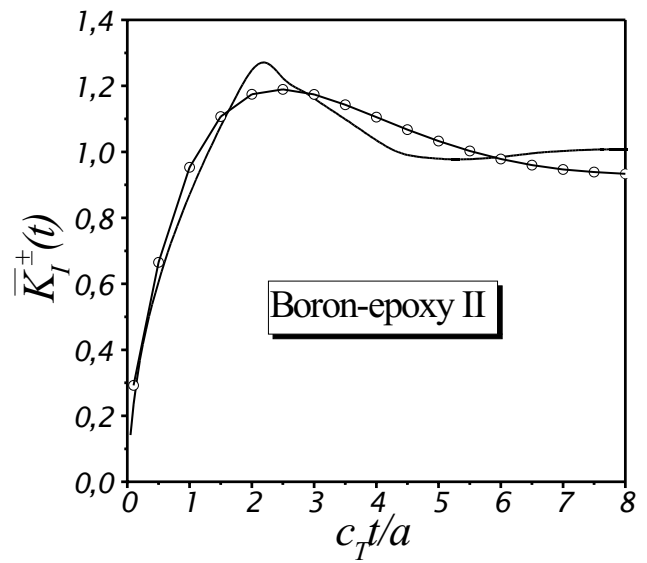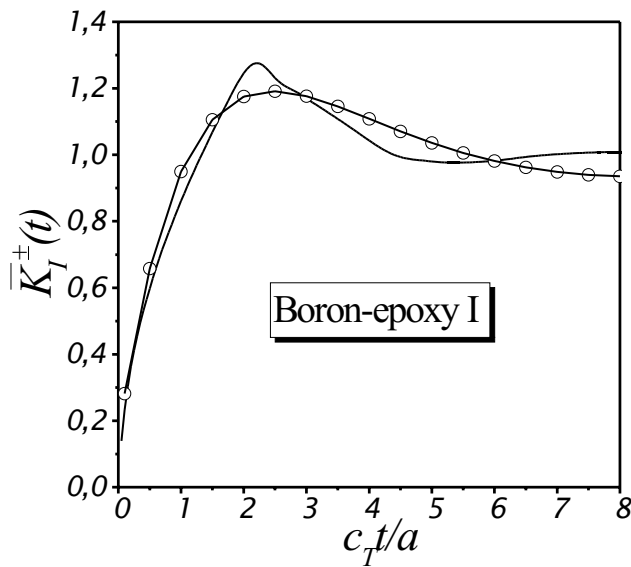
Figure 5 : Normalized $\overline{K}_I^{\pm}$- and $\overline{K}_{II}^{\pm}$-factors

Figure 6 : Normalized $\overline{K}_I^{\pm}$- and $\overline{K}_{II}^{\pm}$-factors

tained by Kassir and Bandyopadhyay (1983). Here, generalized plane stress is assumed and the dimensionless time $c_T t/a$ is used, where $c_T = \sqrt{G_{12}/\rho}$. Numerical calculations are performed by using $K = L = 20$ and a time-step $c_T \Delta t = a/20$. Kassir and Bandyopadhyay (1983) applied a dual integral equation method in the Laplace transform domain in conjunction with an inverse Laplace transform to obtain the time-dependent solutions numerically. The comparision shows that the agreement between the present numerical results and those obtained by Kassir and Bandyopadhyay (1983) is quite satisfactory in the large-time range, while some discrepancies between both results are noted in the small-time range. Presumably, the numerical results of Kassir and Bandyopadhyay (1983) may not be accurate enough in the small-time range, a common fact in the frequency or Laplace transform method. The global behaviors of the normalized elastodynamic stress intensity factors versus the dimensionless time for orthotropic materials considered here are similar to those for isotropic materials as shown in Fig. 2. The dynamic stress intensity factors increase rapidly with increasing time in the small-time range, decrease after reaching a peak, and tend to their corresponding static values in the large-time range.
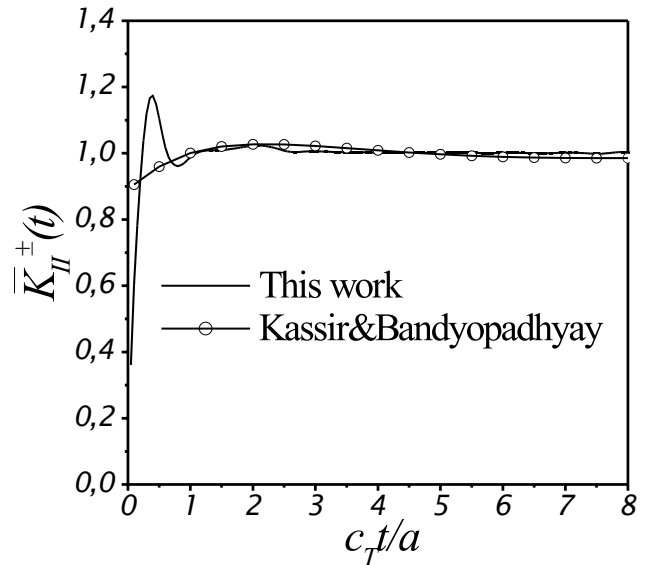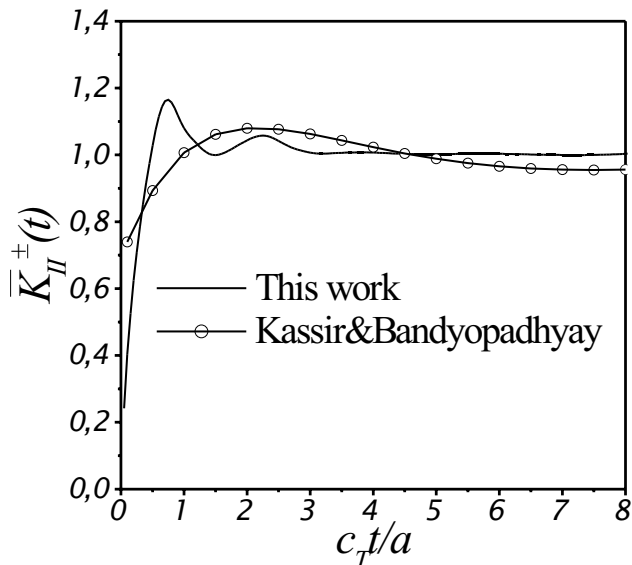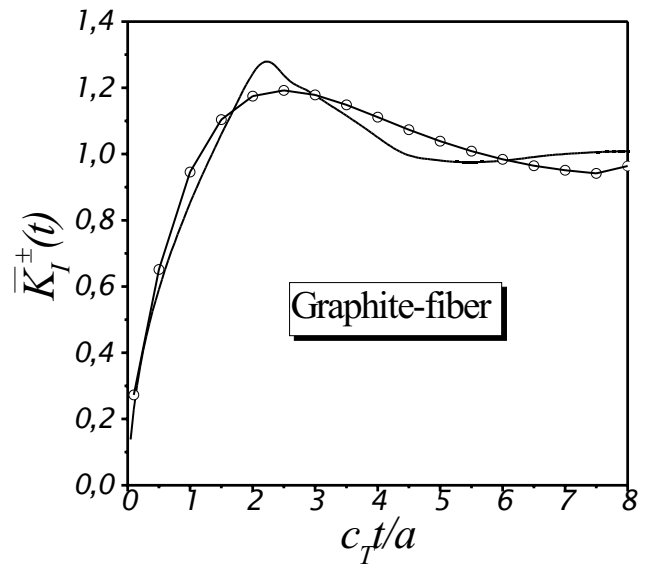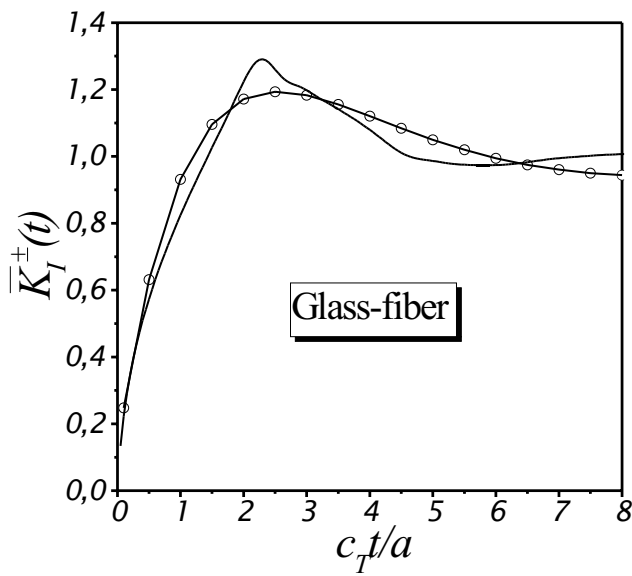
Figure 7 : Normalized $\overline{K}_I^{\pm}$ - and $\overline{K}_{II}^{\pm}$-factors

Figure 8 : Normalized $\overline{K}_I^{\pm}$ - and $\overline{K}_{II}^{\pm}$-factors

To analyze the effects of material anisotropy on the elastodynamic stress intensity factors, additional numerical calculations are carried out, and the used engineering elastic constants are given in Tab. 2. Generalized plane stress is assumed, and an anisotropy parameter $\delta = E_1/E_2$ is introduced for convenience. Also here, $K = L = 20$ and a time-step $c_T \Delta t = a/20$ are applied in the numerical calculations. For simplicity, only the engineering elastic constant E_1 is varied, while the other elastic constants E_2, G_{12} and ν_{12} are kept as constant. This leads to different values for the anisotropy parameter δ. The orthotropic material with $\delta = 10$ corresponds to a graphite-epoxy composite. Fig. 11 shows that the material anisotropy influences both the peak values of the normalized elastodynamic stress intensity factors and the time at which the peaks arise. A smaller value of the anisotropy parameter δ shifts the peaks of the normalized elastodynamic stress intensity factors to a larger value of the dimensionless time $c_T a/t$. The maximum dynamic overshoot of the elastodynamic stress intensity factors over their coppresonding static values is about 30%.
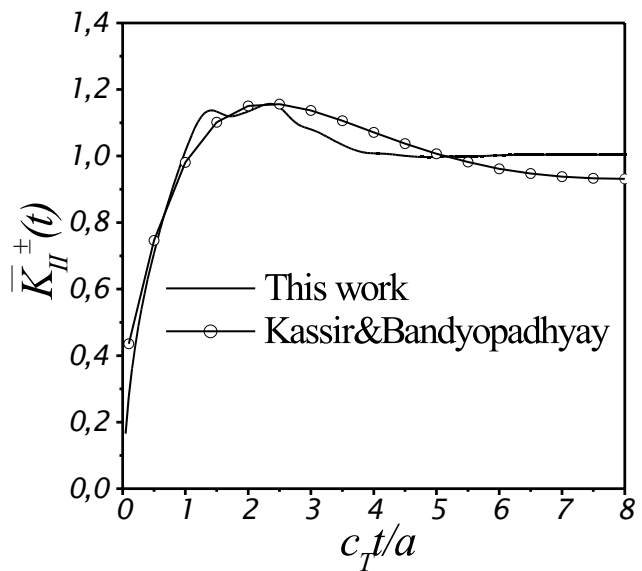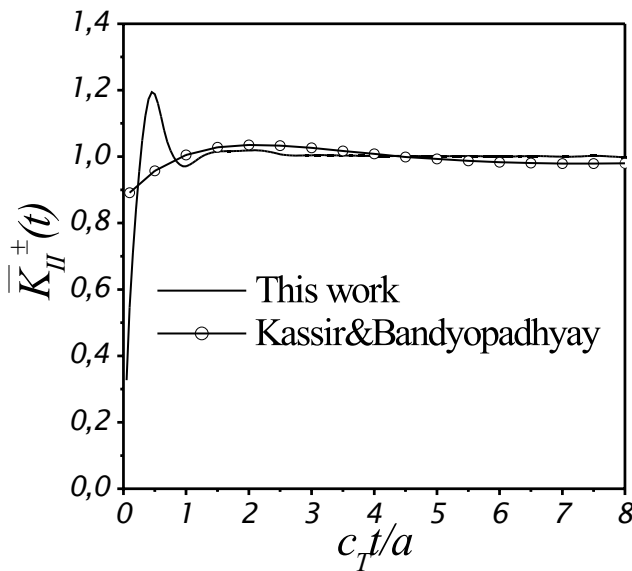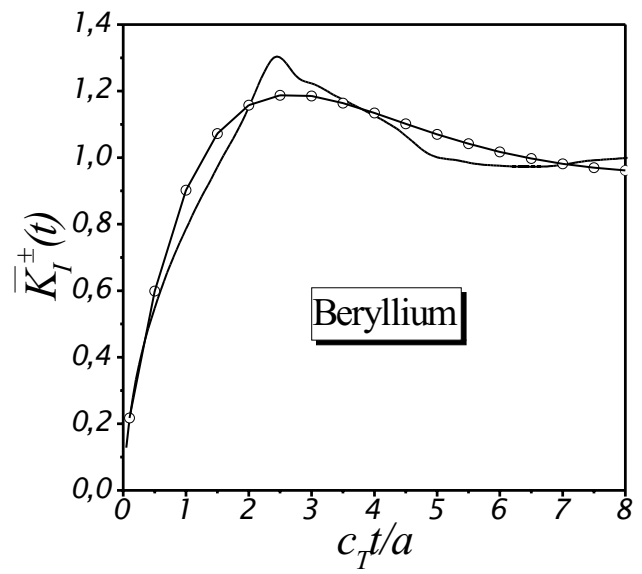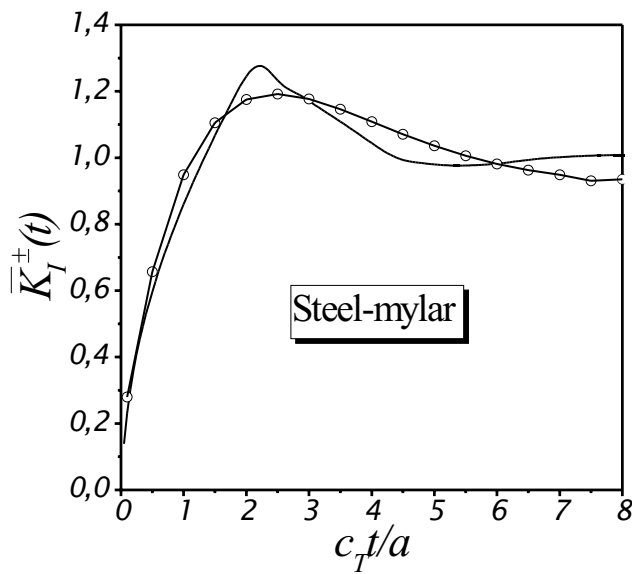
Figure 9 : Normalized $\overline{K}_I^{\pm}$ - and $\overline{K}_{II}^{\pm}$-factors

Figure 10 : Normalized $\overline{K}_I^{\pm}$ - and $\overline{K}_{II}^{\pm}$-factors

7   Conclusions

A 2-D time-domain BIEM for cracked orthortropic solids is presented in this paper. The method has the following advantages:

- The method is especially suited for unbounded domains with straight cracks. The radiation conditions for the displacement and the stress field at infinity are satisfied automatically.

- The formulation is in the time-domain, but no explicit expression of Green's functions in time-

domain is required. The method needs, however, Laplace-domain Green's functions, which should have a simple mathematical structure. The use of Laplace-domain in lieu of time-domain Green's functions in the present time-domain BIEM is made possible by applying the convolution quadrature formula of Lubich (1988a, 1988b, 1994).

- Though the use of a Galerkin method for spatial discretization of the BIEs, only a single integral instead of double or triple integrals needs to be computed numerically. This means that the present spatial

**Table 1** : Engineering elastic constants

Material	E_1 [GPa]	E_2 [GPa]	G_{12} [GPa]	ν_{12}
Boron-epoxy I	224.06	12.69	4.43	0.256
Boron-epoxy II	55.16	170.65	4.83	0.036
Glass-fiber	38.27	9.17	3.72	0.28
Graphite-fiber	173.75	6.89	3.79	0.28
Steel-mylar	181.21	28.30	6.20	0.44
Beryllium	293.19	339.84	112.40	0.24

Table 2 : Elastic constants and anisotropy parameter

E_1 [GPa]	E_2 [GPa]	G_{12} [GPa]	ν_{12}	δ
1.44692	14.4692	5.8565	0.21002	0.1
7.23460	14.4692	5.8565	0.21002	0.5
14.4692	14.4692	5.8565	0.21002	1.0
144.692	14.4692	5.8565	0.21002	10

Galerkin method is computationally not expensiver than the collocation method, which also involves a single integral to be evaluated. In the present method, the arising triple integrals in the system matrix are reduced to a single integral by twice analytical integrations.

- Numerical examples show that the present time-domain BIEM is highly accurate, efficient, and much more stable than the conventional time-domain method using time-dependent Green's functions, which have in anisotropic case very complicated forms and are in general difficult to implement.

- The method can be extended to general anisotropic solids is in a straightforward manner. For cracked solids with general anisotropy and in antiplane strain, the corresponding time-domain traction BIEM has been presented by Zhang (2000a).
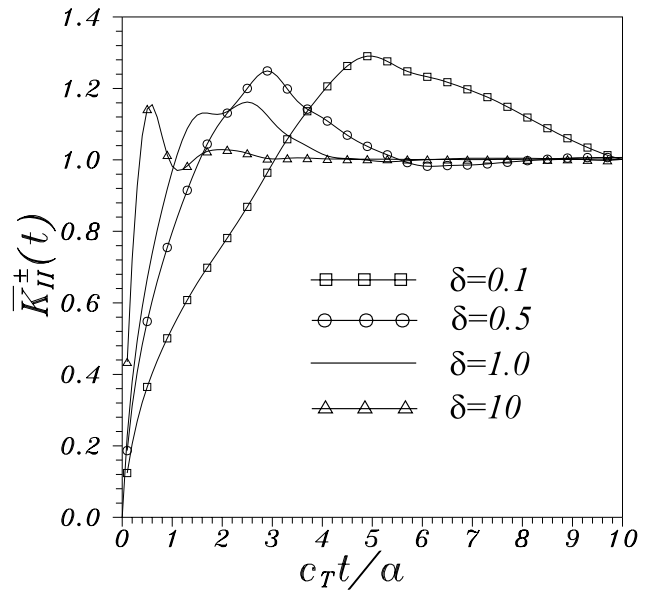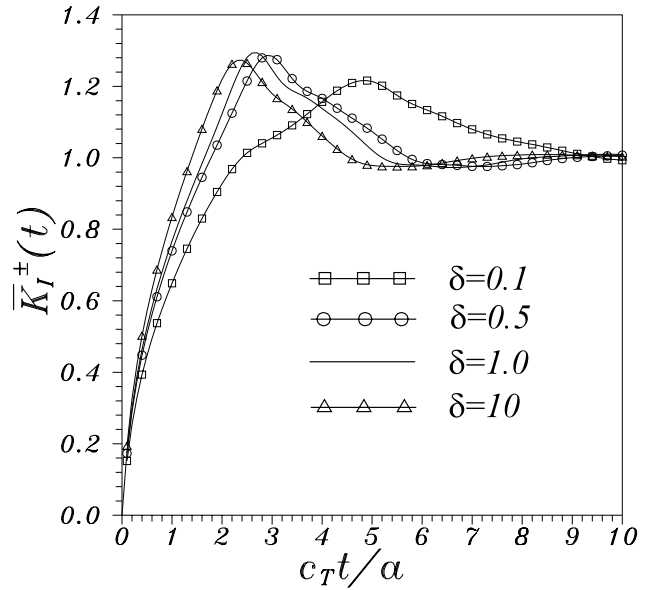
Figure 11 : Effects of the anisotropy parameter δ on $\overline{K}_I^\pm$- and $\overline{K}_{II}^\pm$-factors

The extension of the present time-domain BIEM to general anisotropic solids with cracks, and to finite domains is in progress and the corresponding results will be reported in future.

References

Abramowitz, M.; Stegun, I. A. (1972): *Handbook of mathematical functions*. Dover Publications, New York.

Achenbach, J. D. (1973): *Wave propagation in elastic solids*. North-Holland, Amsterdam/New York.

Albuquerque, E. L.; Sollero, P. (1998): The boundary element method applied to transient dynamic anisotropic problems. In: A. J. Kassab; C. A. Brebbia; M. Chopra (eds) *Proc. Boundary Element Method XX*, WIT Press, UK, pp. 617–624.

Albuquerque, E. L.; Sollero, P.; Aliabadi, M. H. (1999a). The dual boundary element method applied to dynamic fracture mechanics in anisotropic solids. In: M. H. Aliabadi (ed) *Boundary Element Techniques*, Queen Mary and Westfield College, University of London, UK, pp. 23–29.

Albuquerque, E. L.; Sollero, P.; Aliabadi, M. H. (1999b): Computation of dynamic stress intensity factors in anisotropic materials using the boundary element method. In: *20th Ibero-Latin-American Conf. for Comput. Meth. in Engng. - XX CILAMCE)*, 3-5 November 1999, Sao Paulo, Brazil.

Albuquerque, E. L.; Sollero, P.; Aliabadi, M. H. (2000): The boundary element method applied to time dependent problems in anisotropic materials. *Int. J. Solids Struct.*, submitted for publication.

Albuquerque, E. L.; Sollero, P.; Fedelinsky, P. (2000): Analysis of anisotropic dynamic crack problems using the dual reciprocity boundary element method in Laplace domain. *Computers & Structures*, submitted for publication.

Beskos, D. E. (1997): Boundary element methods in dynamic analysis: part II (1986-1996). *Appl. Mech. Rev.*, vol. 50, pp. 149-197.

Dominguez, J.; Sáez, A. (1998): Boundary element analysis of 3-D dynamic crack problems in isotropic and transversely isotropic solids. In: *Fourth Word Congress on Computational Mechanics*, June 29 - 2 July 1998, Buenos Aires, Argentina.

Hwang, C.; Geubelle, P. H. (2000): A spectral scheme to simulate dynamic fracture problems in composites. *CMES:Computer Modeling in Engineering & Sciences*, vol. 1 no. 4, pp. 45–56.

Hirose, S. (1999): Dynamic analysis for a crack in anisotropic elastic solid (in Japanese). In: *JASCOME Proc. of BTEC-99*, vol. 16, pp. 13-17.

Hirose, S.; Wang, C.-Y.; Achenbach, J. D. (2000): Boundary element method for elastic wave scattering by a crack in an anisotropic solid. In: *20th Int. Congress Theoret. Appl. Mech. ICTAM 2000*, 27 August - 2 September 2000, Chicago, USA.

Kassir, M. K.; Bandyopadhyay, K. K. (1983): Impact response of a cracked orthotropic medium. *ASME J. Appl. Mech.*, vol. 50, pp. 630–636.

Kögl, M.; Gaul, L. (2000): A 3-D boundary element method for dynamic analysis of anisotropic elastic solids. *CMES:Computer Modeling in Engineering & Sciences*, vol. 1 no. 4, pp. 27–43.

Lubich, C. (1988a): Convolution quadrature and discretized operational calculus. I. *Numerische Mathematik*, vol. 52, pp. 129-145.

Lubich, C. (1988b): Convolution quadrature and discretized operational calculus. II. *Numerische Mathematik*, vol. 52, pp. 413–425.

Lubich, C.; Schneider, R. (1992): Time discretization of parabolic boundary integral equations. *Numerische Mathematik*, vol. 63, pp. 455–481.

Lubich, C. (1994): On the multistep time discretization of linear initial-boundary value problems and their boundary integral equations. *Numerische Mathematik*, vol. 67, pp. 365–389.

Mattsson, J. (1996): *Modeling of scattering by cracks in anisotropic solids - Application to ultrasonic detection*. Ph.D. Thesis, Div. Mech., Chalmers University of Technology, Göteborg, Sweden.

Nishimura, N.; Kobayashi, S.; Kishima, T. (1986): A BIE analysis for wave propagation in anisotropic media. In: M. Tanaka; C. A. Brebbia (eds) *Boundary Elements VIII*, Springer-Verlag, pp. 425-434.

Nishimura, N.; Kobayashi, S.; Takeuchi, T. (1995): Solution of 2D anisotropic elastodynamic problems by BIEM (in Japanese). In: *JACOME Proc. of BTEC-95*, vol. 5, pp. 7–10.

Sáez, A.; Dominguez, J. (1999a): Scattering of elastic waves by cracks in 3-D transversely isotropic solids. In: M. H. Aliabadi (ed) *Boundary Element Techniques*, Queen Mary and Westfield College, University of London, UK, pp. 455–463.

Sáez, A.; Dominguez, J. (1999b): BEM analysis of wave scattering in transversely isotropic solids. *Int. J. Numer. Meth. Engng.*, vol. 44, pp. 1283–1300.

Sáez, A.; Dominguez, J. (2000): Far field dynamic Green's functions for BEM in transversely isotropic

solids. *Wave Motion*, vol. 32, pp. 113–123.

Sáez, A.; Dominguez, J. (2001): Dynamic crack problems in three-dimensional transversely isotropic solids. *Eng. Anal. Boundary Elem.*, vol. 25, pp. 203–210.

Shiah, Y. C.; Tan, C. L. (2000): Fracture mechanics analysis in 2-D anisotropic thermoelasticity using BEM. *CMES: Computer Modeling in Engineering & Sciences*, vol. 1, pp. 91–99.

Sih, G. C.; Paris, P. C.; Irwin, G. R. (1965): On cracks in rectlinearly anisotropic bodies. *Int. J. Fract.*, vol. 1, pp. 189-203.

Thau, S. A.; Lu, T. H. (1971): Transient stress intensity factors for a finite crack in an elastic solid caused by a dilatational wave. *Int. J. Solids Struct.*, vol. 7, pp. 731-750.

Wang, C.-Y.; Achenbach, J.D. (1992): A new look at 2D time-domain elastodynamic Green's functions for general anisotropic solids. *Wave Motion*, vol. 16, pp. 389–405.

Wang, C.-Y.; Achenbach, J.D. (1993): A new method to obtain 3-D Green's functions for anisotropic solids. *Wave Motion*, vol. 18, pp. 273–289.

Wang, C.-Y.; Achenbach, J.D. (1994): Elastodynamic fundamental solutions for anisotropic solids. *Geophys. J. Int.*, vol. 118, pp. 384–392.

Wang, C.-Y.; Achenbach, J.D. (1995): Three-dimensional time-harmonic elastodynamic Green's functions for anisotropic solids. *Proc. R. Soc. Lond.* A, vol. 449, pp. 441–458.

Wang, C.-Y.; Sáez, A.; Achenbach, J.D. (1995): 3-D elastodynamic Green's functions for BEM applications to anisotropic solids. In: D. F. Parker; A. H. England (eds) *Proc. IUTAM Symposium on Anisotropy, Inhomogeneity and Nonlinearity in Solid Mechanics*, Kluwer Academic Publisher, The Netherlands, pp. 307–320.

Wang, C.-Y.; Achenbach, J. D.; Hirose, S. (1996): Two-dimensional time domain BEM for scattering of elastic waves in solids of general anisotropy. *Int. J. Solids Struct.*, vol. 33, pp. 3843–3864.

Zhang, Ch.; Savaidis, A. (1999): Time-domain BEM for dynamic crack analysis. *Mathematics and Computers in Simulation*, vol. 50, pp. 351-362.

Zhang, Ch. (2000a): Transient elastodynamic antiplane crack analysis in anisotropic solids. *Int. J. Solids Struct.*, vol. 37, pp. 6107–6130.

Zhang, Ch. (2000b): A 2-D time-domain BIEM for dynamic analysis of cracked orthotropic solids. In: S. N. Atluri; F. W. Brust (eds) *Advances in Computational Engineering & Sciences*, Tech Science Press, USA, vol. II, pp. 1246–1251.

Zheng, T.; Dravinski, M. (2000): Scattering of elastic waves by a 3D anisotropic basin. *Earthquake Engng. Struct. Dyn.*, vol. 29, pp. 419–439.